How swelling, crosslinking, and aging affect drop pinning on lubricant-infused, low modulus elastomers

*Zhuoyun Cai and Jonathan T. Pham**

Department of Chemical and Materials Engineering, University of Kentucky, Lexington, KY 40506, USA.

Keywords: *soft elastomers, wetting, slippery lubricant-infused surfaces, drop pinning, self-lubrication*

ABSTRACT Soft, slippery surfaces have gained increasing attention due to their wide range of potential applications, for example in biomaterials, self-cleaning, anti-fouling, liquid collection, and more. One approach to prepare a soft, slippery surface is by swelling a crosslinked polymer network with a lubricant. However, an understanding of how swelling and crosslinking relate to slippery properties is still underdeveloped for low modulus elastomers. We study when a water drop sticks or slides on a vertical, silicone oil-swollen polydimethylsiloxane (PDMS) elastomer as a function of the degree of crosslinking and the degree of swelling. Our results indicate that the critical water drop volume required for sliding is strongly controlled by the degree of swelling; higher swelling leads to lower critical drop volumes. In addition, we demonstrate that highly swollen surfaces, and not lightly swollen surfaces, recover their slippery behavior during an aging process after they are rinsed with

water. This is likely associated with regeneration of an oil-layer on the surface coming from the bulk substrate, illustrating the durability of lubricant-swollen elastomers for practical uses.

Introduction

Water-repellent surfaces have attracted significant attention due to their diverse range of applications, from self-cleaning to anti-fouling. One route to achieve water repellency is by introducing small structures on a surface, which reduces the water-surface contact area by forming air pockets under the drop. This is commonly known as the "lotus effect", and has been the foundation for developing superhydrophobic[1,2] and superoleophobic surfaces.[3–5] However, the liquid-repellent properties rely on trapped air pockets, which can be impaled by liquid due to high pressures.[6] One approach to overcome this challenge is by using lubricant-infused porous substrates (SLIPS); these are usually micro- or nano-structured surfaces infiltrated with a lubricant.[7–9] When a water drop is placed on SLIPS, the infused lubricant separates the water drop from the substrate to make a liquid-liquid interface, allowing water to slide easily along the surface. By using appropriate lubricants,[10,11] SLIPS can also be designed to repel low surface tension liquids, including alkanes, alcohols and ketones.[7] To date, SLIPS have been developed for self-cleaning,[12] anti-icing,[13] anti-frosting,[14] anti-biofouling,[15] and preventing blood clotting.[16] However, one of the ongoing challenges is related to lubricant loss over time. Lubricant is typically held within the microstructured surface by capillary forces; however, lubricant is pulled out by water drops. Hence, many situations can lead to lubricant-depletion, including drops condensation,[17] moving drops,[10] gravitational drainage[18] and evaporation.[19]

In an attempt to minimize lubricant-depletion, a crosslinked polymer network can be used to hold the lubricant inside the substrate. In this case, the polymer network is infused with a lubricant, creating a swollen elastomer. Lubricant-swollen elastomers can have excellent liquid-repellent properties, which are generally afforded by a lubricant layer that persists on the polymer surface.[20–22] In contrast to traditional SLIPS, the lubricant layer on swollen elastomers can display syneresis,[21–23] dramatically increasing the slippery function of the surfaces. Aside from liquid repellency, soft substrates offer flexibility, stretchability, and biocompatibility, making them potential candidates for applications in cell culture and biomedical devices,[24–26] soft robotics,[27] and electronic skins.[28,29] Although many lubricant-swollen elastomers rely on a lubricant layer oil at the topmost surface to maintain the slippery properties, recent studies suggest that swollen elastomers can also maintain slippery behavior even when no lubricant layer is clearly observable on the surface.[30,31] This is likely the result of lubricant being pulled out from the polymer network at the contact line of a water drop or a solid contact.[32–35] Although crosslinking effects have been considered for wetting of infused elastomers, they are usually relatively stiff and swollen to saturation (equilibrium).[23,36–38] Hence, it is not well known how the degree of crosslinking of the polymer network , together with the swelling ratio, govern the ability for water drops to slide on low modulus, swollen elastomers. Therefore, a systematic analysis that examines when water drops stick or slide on lubricant-swollen, low modulus elastomers would be beneficial for developing water-repellent soft coatings.

Here we investigate how the degree of crosslinking and the degree of swelling controls when a drop is pinned or slides on a soft silicone elastomer. Our study focuses on softer materials with dry shear moduli ranging from ~5 to 82 kPa (and swollen shear moduli ranging from ~1 to 27 kPa). With gravity as the driving force, we quantify the critical volume required for a drop to slide on these surfaces when held vertically. Interestingly, for dry polymer networks, the critical volume is nearly independent of the degree of crosslinking below a certain level. For lubricant-infused elastomers, we find that the critical volumes are strongly dependent on the degree of swelling and only moderately related to the crosslinking. By running through several rinsing cycles, we find that highly swollen samples can recover and re-lubricate their surface after a few days, while re-lubrication is not observed for intermediately swollen surfaces. Our findings on water drop sliding and pinning aim to provide insight for designing soft, water-repellent, swollen surfaces.

Results and discussion

Pinning/sliding on dry elastomers

Before investigating how a drop sticks on a swollen elastomer, we first study the pinning of water drops on dry surfaces with different crosslinking. Here, dry elastomers are defined as those without any uncrosslinked chains (which are also known as free chains or infused fluid molecules). To control the degree of crosslinking, we prepare PDMS elastomers from Sylgard 184 with mixing ratios of 30:1, 40:1, 50:1 and 60:1 by weight of the base to crosslinking agent, where 30:1 and 60:1 are the highest and lowest modulus materials, respectively. These as-prepared samples contain uncrosslinked chains that are not connected to polymer network

during curing, where the amount of free chains is dependent on the base/crosslinker mixing ratio; the amount of free chains is almost ~60% for the 60:1 ratio.[39] Consequences of uncrosslinked chains in silicone elastomers have been investigated in the context of adhesion,[34,35] osmocapillary phase-separation,[40] surface tension[41] and droplet dynamics.[42] These studies reveal how uncrosslinked chains can lead to significant macroscopic effects, such altering drop sliding velocities[33] or modifying the contact line geometries.[34] Hence, uncrosslinked chains need to first be removed to exclude their effects and to better control our material systems. To extract free chains from our as-prepared materials, the samples are swollen in a good solvent to let free chains migrate out. Details of the process are described elsewhere[39] and in the methods section. Upon extracting free chains, the polymer surfaces are considered as dry elastomers.

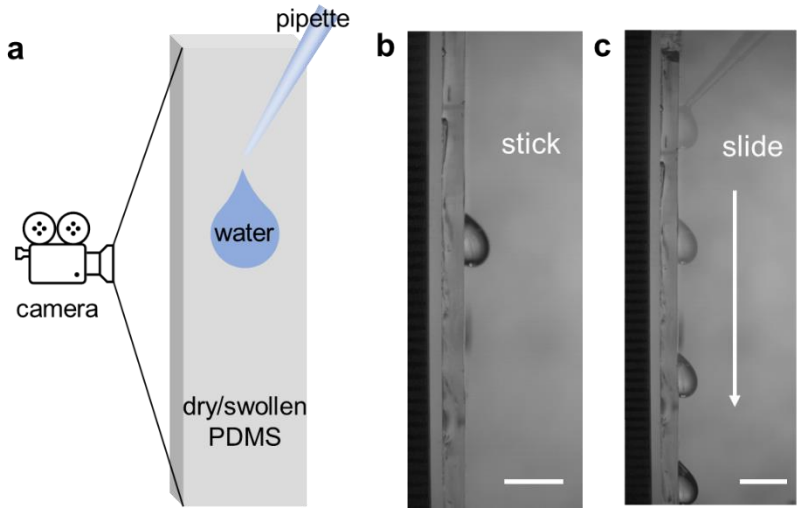

Figure 1. A water drop is deposited on a vertical PDMS elastomer. (a) A schematic of experimental setup. (b) An image of a water drop sticking to a surface and (c) of a water drop sliding on the surface. Note that four images are overlaid in (c) to illustrate drop sliding. Scale bars: 5 mm.

To study drop pinning, the samples are vertically placed in a chamber with a relative humidity of 70% to 75%. Water drops of different volumes are then placed on the surface by micropipette, and a side-view camera is used to record drop motion (Figure 1a). Drop-surface interactions (related to adhesion) drive the drop to stick, while gravity (related to drop size) drives the drop to slide. Hence, two main outcomes exist: A water drop can either slide (Movie 1) or stick (Movie 2) on the surface (Figure 1b, c). We note that a third case can also be observed, where the water drop initially slides slowly and then sticks on surface. One reason for this mixed case may be that initial sliding occurs due to the kinetic energy introduced when the drop is placed; once the kinetic energy is consumed by friction, the drop sticks on the surface. For simplicity, we describe drop behaviors as either a sliding case or a sticking case, and recognize the third case (sliding first followed by sticking) as the sticking state.

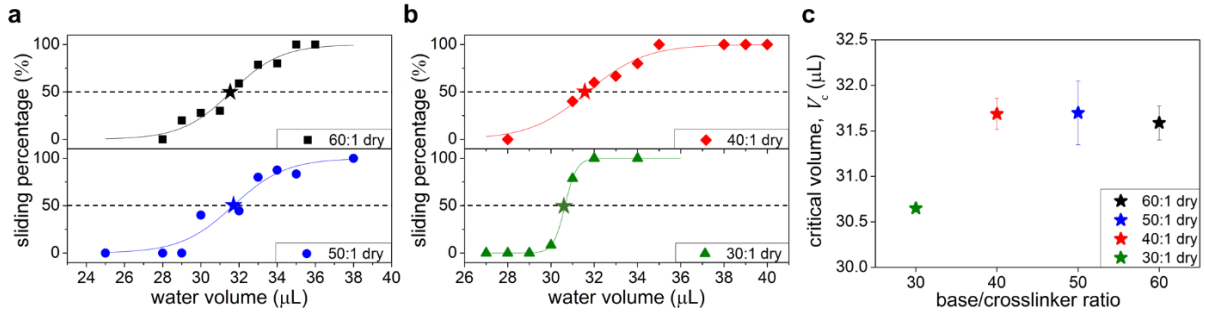

Figure 2. Water drop sliding percentage on dry surfaces with base/crosslinker ratios of (a) 60:1 and 50:1, and (b) 40:1 and 30:1. The horizontal dashed line represents the sliding percentage of 50%. The star shows the 50% point of our fit, which is taken as V_c. Each data point includes at least 5 drops. (c) The critical volume V_c as function of base/crosslinker ratio for dry samples. The error bars denote standard error on x_0 of the Boltzmann fit.

For dry surfaces with different crosslinking, we plot the percentage of drops that slide as a

function of drop volume (Figure 2). This approach is used to present the data because we find that even on the same samples, some drops of the same volume slide while others stick. For example, each data point includes at least 5 drops at that particular volume. If 4 out of 5 drops slide, this equates to an 80% sliding percentage (Movie 3). Hence, by plotting the percentage of drops that slide, we incorporate both potential error as well as the sensitivity to how drop volume controls drop sliding. As illustrated in Figure 2a and 2b for the four crosslinking ratios, all drops stick (0%) below a certain volume while all drops slide (100%) above a certain volume, with a transition region that exists in between. To quantify a critical volume (V_c), we define it as when 50% of the deposited drops slide down the surface. Critical volumes are obtained by fitting the sliding percentage data with a Boltzmann function, $y = \frac{A_1 - A_2}{1+e^{(x-x_0)/dx}} + A_2$, where the 50% threshold of y is obtained at the x, y point $(x_0, (A_1 + A_2)/2)$. In our case, y represents the sliding percentage and x represents the water volume, and $A_1$and A_2 are set to 0% and 100%, respectively; after fitting, x_0 represents the critical volume. This 50% point is noted as a star in Figure 2. As shown in Figure 2c, V_c for 30:1 substrates (dry shear modulus G_{dry}~82 kPa) is around ~30.5 μL, while V_c for the 40:1 (G_{dry}~21 kPa), 50:1 (G_{dry}~12 kPa), and 60:1 (G_{dry}~5 kPa) (Figure S1, Table 1) mixing ratios are around ~31.5 μL. It appears that V_c is independent of crosslinking for the 40, 50, and 60:1 dry samples. The 40, 50, and 60:1 samples display a similar plot shape in the transition region, while the 30:1 substrates have a steeper transition. This may suggest that the 30:1 substrates are sufficiently stiff, such that their drop-surface behaviors are different than the softer mixing ratios. In addition, we initially hypothesized that softer samples (e.g. 60:1) require a higher V_c because they have larger wetting ridges. A wetting ridge is an out-of-plane substrate deformation that occurs at the drop

periphery due to a balance of surface and elastic forces; the water drop surface tension drives the ridge to form while elastic restoring force of the polymer network resists ridge formation.[43–45] In general, softer substrates have a weaker elastic restoring force, leading to larger wetting ridges that would hinder drop motion.[46] In a previous study, we found that the wetting ridge heights for a static water drop range from ~6.5 μm for a 60:1 dry PDMS surface down to ~0.5 μm for a dry 30:1 surface.[32] However, one possible reason that V_c is not related to the degree of crosslinking may be due to the introduction of the different modulus. If we consider that a drop slides down a surface by moving a solid wetting ridge,[47,48] then the wetting ridge height and wetting ridge stiffness (i.e. modulus) both play a role. Since the wetting ridge height is inversely proportional to modulus,[32,49] this may lead to similar V_c on soft samples.

Sliding on swollen elastomers

We now turn our attention to water drop pinning/sliding on oil-infused (swollen) elastomers. Trimethylsiloxy-terminated linear silicone oil (M_w: 770 g/mol) is implemented as our swelling fluid. This oil is chosen because it has good affinity with the PDMS network, such that the network can be highly swollen, and it is a non-volatile fluid, which allows the material to remain stable over time. To characterize the amount of oil infused into each network, the degree of swelling is quantified by weight and defined as $Q = w_s/w_d$, where w_d is the weight of the dry sample and w_s is the weight of the sample after swelling. We note that the modulus of swollen elastomers depends on both the initial base/crosslinker mixing ratio as well as Q. For all mixing ratios, the moduli decrease with increasing swelling (Figure S1).[32] Moreover, as the base/crosslinker ratio is increased from 30:1 to 60:1, the saturated degrees of swelling (i.e.,

maximum swelling, $Q_{\max}$) increase from $Q_{\max} \approx 4.1$ (30:1) to $Q_{\max} \approx 13.1$ (60:1) (Figure 3). This is not surprising because an elastomer with less crosslinking (e.g. 60:1) can expand and absorb more oil into the polymer network. For the following studies, we prepare samples that are near their saturated swelling ratio, as well as one at an intermediate swelling ratio. The shear moduli are presented in Table 1, which are consistent with prior measurements.[32]

Table 1: Swelling ratio (Q, by weight) and shear storage modulus for the four different mixing ratios of Sylgard 184 used in this study.

60:1		50:1		40:1		30:1	
Q	G (kPa)	Q	G (kPa)	Q	G (kPa)	Q	G (kPa)
1.0 (dry)	5.1 kPa	1.0 (dry)	12 kPa	1.0 (dry)	21 kPa	1.0 (dry)	82 kPa
3.4	2.5 kPa	7.0	4 kPa	3.1	10 kPa	3.2	27 kPa
13.1	0.9 kPa	9.4	2 kPa	5.5	8.2 kPa	4.1	25 kPa

In the same approach used for dry elastomers, we measure V_c on swollen substrates with the four base/crosslinker mixing ratios at different Q. Since an oily layer at the surface can play a role in drop wetting,[20–23] it is important have a consistent testing surface. In the literature, this can be done by wiping the surface prior to placing drops;[21,50] however, for our very soft, and sometimes sticky samples, it is challenging to wipe without damage. Therefore, all swollen samples are rinsed with excess water to remove residual oil that may be on the surface, just before drop pinning experiments. In general, we find that V_c decreases with increasing Q, regardless of the degree of crosslinking (Figures 3a-3b). For example, V_c on the 30:1 samples are ~31.5, 6.0, and 1.5 μL for $Q = 1$ (dry), 3.2 and $Q_{\max} = 4.1$ (saturated), respectively. This demonstrates that surfaces become more slippery when more oil is swollen into the network. For the 40, 50, and 60:1 samples, the same trend of decreasing V_c with increasing Q is observed, but with quantitatively different values (Figures 3c). In particular, we can compare the cases at

Q_{max} for the different mixing ratios; the V_c are 1.5, 5.7, 6.1, 5.6 µL for the saturated 30:1, 40:1, 50:1 and 60:1 substrates, respectively. This implies that for saturated networks, V_c is not strongly correlated to crosslinking at a 40:1 mixing ratio and softer. In a consistent fashion to the dry samples in Figure 2c, the 30:1 sample has a lower V_c than the 40, 50, and 60:1 samples.

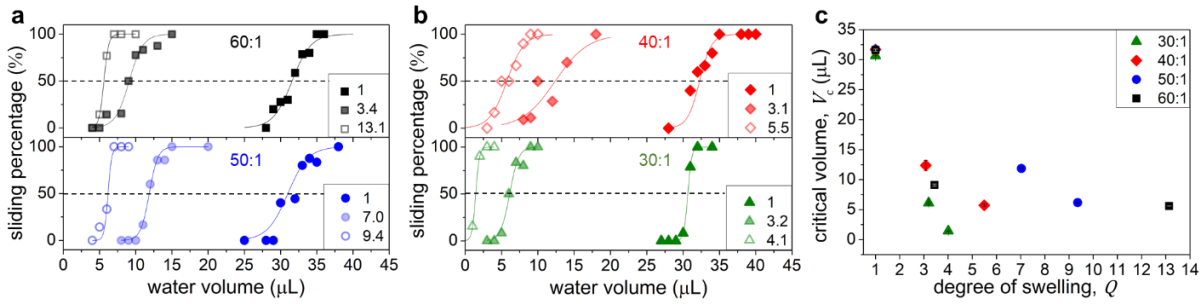

Figure 3. Water drop sliding percentage on surfaces with various degrees of swelling for (a) 60:1 and 50:1 samples and for (b) 40:1 and 30:1 samples. The horizontal dashed line represents the sliding percentage of 50%. (c) The critical volume V_c as a function of degree of swelling Q for the 30:1, 40:1, 50:1 and 60:1 samples.

Calculation of critical drop volume

Water drop pinning on a vertical surface usually results from a competition between the drop interaction with the substrate balanced by the gravitational force acting on the drop. For a water drop with volume V, the gravitational force is:

$$F_g = \rho V g \quad (1)$$

where ρ is the density of water and g is the gravitational acceleration. Gravity drives the water drop to slide while adhesion and capillarity pin the drop in place. The critical pinning force can be calculated as:[51,52]

$$F_p = k\gamma D(cos\theta_R - cos\,\theta_A) \quad (2)$$

where the k is a constant related to the shape of the drop, γ is the water surface tension, D is the contact diameter, and θ_R and θ_A are the receding and advancing contact angles, respectively. When a small drop sticks on the surface, gravity cannot overcome the pinning force (i.e., $F_g < F_p$). As the volume of the drop is increased, it eventually reaches a critical volume V_c, at which point gravity is sufficiently high to overcome the pinning force. Theoretically, V_c occurs when $F_g = F_p$. Thus, V_c can be approximated by combining Equations 1 and 2 as:

$$V_c = \frac{k\gamma D(cos\theta_R - cos\,\theta_A)}{\rho g} \tag{3}$$

The contact diameter D varies with the drop volume, with larger drops having larger D. To simplify the relationship between V and D, we assume the two factors follow the function:

$$V = aD^3 \tag{4}$$

where a is a constant. By combining and rearranging Equations 3 and 4, a prediction for V_c becomes:

$$V_c = \left[\frac{k\gamma(cos\theta_R - cos\theta_A)}{a^{\frac{1}{3}}\rho g}\right]^{\frac{3}{2}} \tag{5}$$

Since the drop is not a spherical cap due to gravity, we use a as an empirical constant. To determine a for our material systems, we test a range of drops with different V (1 μL ~40 μL) when they stick on either dry or swollen surfaces and measure D. Figure 4 shows a plot of V as a function of D^3. The volume V follows a linear function with D^3, consistent with Equation 4, regardless of the degrees of crosslinking and swelling; an a value of 0.17 is obtained by fitting a line and taking the slope.

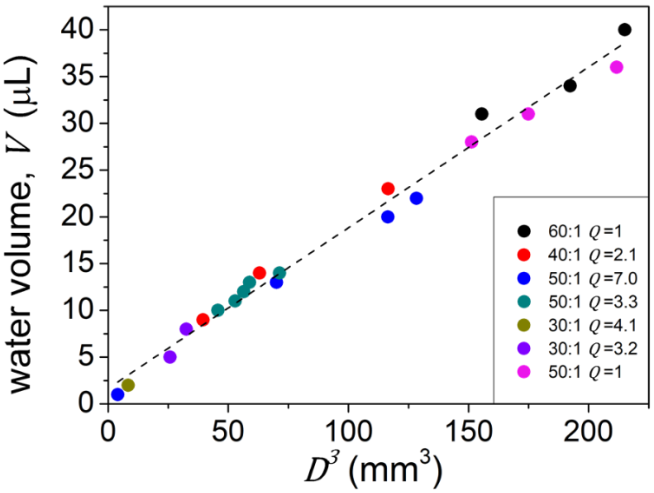

Figure 4. Water volume V as a function of contact diameter cubed D^3 on different elastomers. The dashed line is a linear fit of all data points with a resulting slope of 0.17.

The advancing (θ_{A}) and receding (θ_{R}) contact angles are measured by using an automatic dispensing system. The dispensing system outputs and inputs water on the sample surface with a constant inject/withdraw speed (0.05 μL/s). The advancing angles are taken as the apparent contact angle when the contact line depins and expands during water injection, while the receding angles are obtained when the water contact line depins and start moving backwards during water withdrawal.[30,53,54] Figure 5 shows plots of advancing and receding contact angles on samples with different degrees of crosslinking and different Q. As suggested by Figure 3, the surfaces are more slippery with higher Q; that is, V_{c} is smaller for surfaces with higher Q. Hence, the contact angle hysteresis ($CAH = \theta_{\mathrm{A}} - \theta_{\mathrm{R}}$), which offers information on drop-surface adhesion, is also expected to be smaller for higher Q. This is confirmed in Figure 5, where the smallest CAH for a given base/mixing ratio is observed at Q_{max}. The CAH increases with decreasing Q, and are largest when samples are dry. Moreover, we point out that the 30:1 substrates (Figure 5a) display the smallest CAH at Q_{max}, while CAH for saturated 40:1, 50:1

and 60:1 are larger. This is consistent with the V_c results in Figure 3, suggesting that 30:1 samples have slightly different properties.

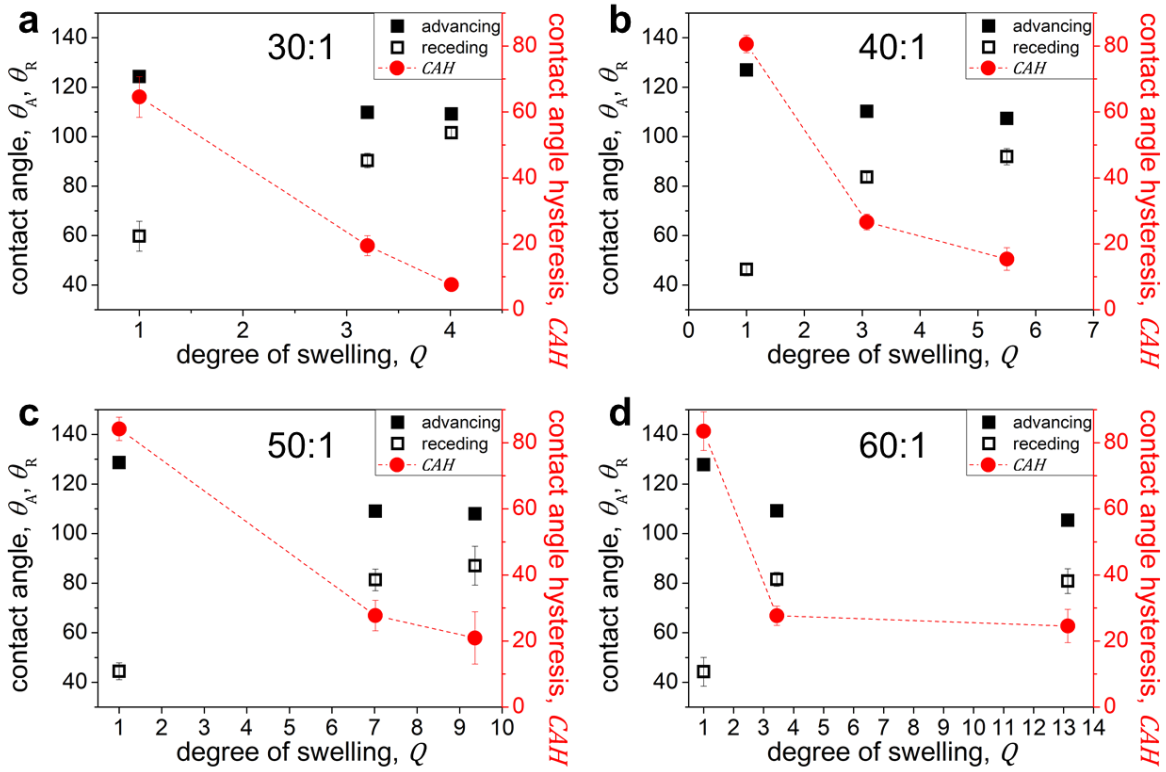

Figure 5. Advancing and receding contact angles, as well as the contact angle hysteresis of water on (a) 30:1, (b) 40:1, (c) 50:1 and (d) 60:1 samples with different degrees of swelling from dry to saturated.

To compare Equation 5 to our experiments, we calculate the critical volume V_c by using measured θ_R and θ_A, a value of $a = 0.17$, and known values for ρ, g and γ for water. This leaves the parameter k, which depends on the geometry of the drop and can be difficult to determine. In literature, k has been reported to be in a range of 0.5 to π/2 (1.57).[55–57] Since we do not have a way to determine k, and because it is not yet consistent in literature, we assume that $0.5 \leq k \leq \frac{\pi}{2}$. In Figure 6, the experimental data for V_c is plotted alongside calculated

values from Equation 5 for $k = 0.5$ (red dashed line) and for $k = 1.57$ (black dashed line). Our results are close to $k = \pi/2$ but lie within these two regions, indicating that Equation 5 is consistent with experimental V_c for our substrates, including both dry and swollen elastomers.

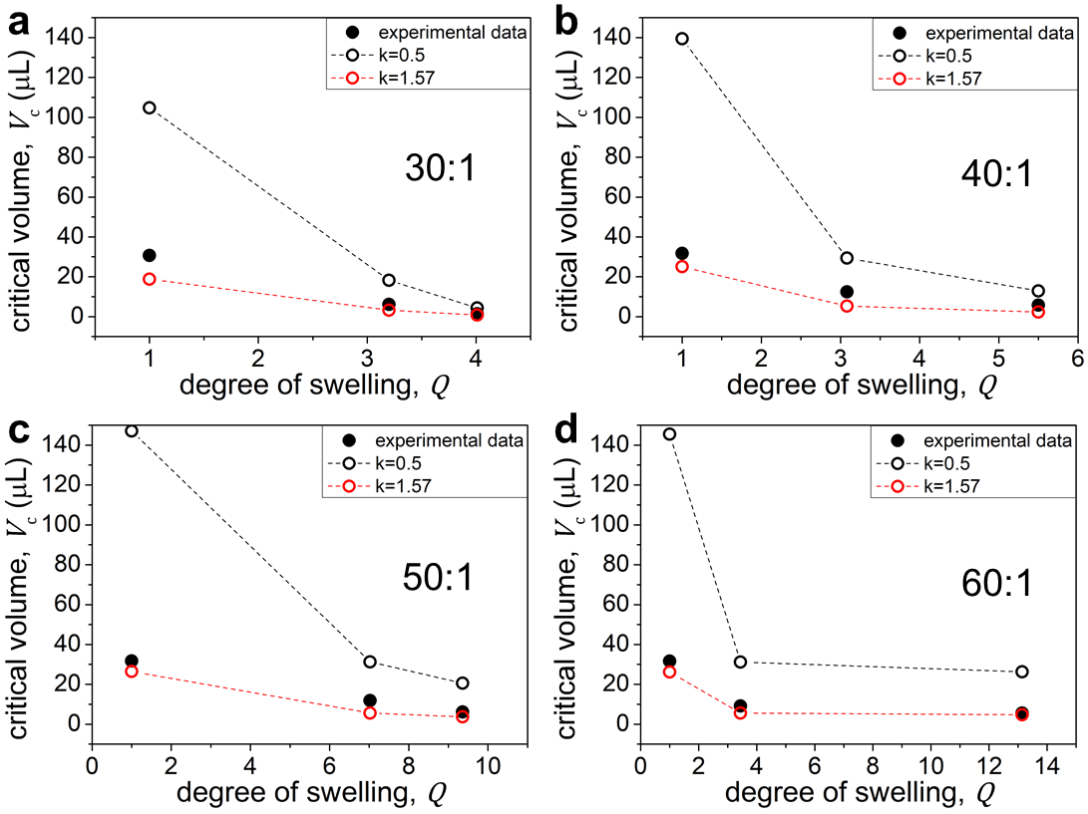

Figure 6. Plots of the experimental data for V_c vs. Q (filled black data points) overlaid with calculated values from Equation 5 for (a) 30:1, (b) 40:1, (c) 50:1 and (d) 60:1 swollen elastomers. The open black circles and dashed lines are the calculated from Equation 5 with k = 0.5, and the open red circles and dashed lines for k = 1.57.

Rinsing, aging and re-lubrication

Maintaining slippery properties is a challenge for lubricant-infused surfaces,[17,58–60] because lubricant can be depleted by rinsing. In this section, we investigate the rinsing, aging, and re-lubrication behavior of our swollen samples. To rinse a surface, 500 mL of deionized water is

steadily poured onto the surface. During this rinsing cycle, extra oil on the surface is removed. Afterwards, water drops are then deposited onto the surface to determine V_c. Moreover, we continue to measure V_c for several days after rising to examine the effects of aging and re-lubrication. For aging, samples are left in an ambient environment (closed petri dish) without applying any external energy. This rinsing and aging process is conducted over multiple rinsing cycles on the same surface, which allows us to investigate drop pinning/sliding before and after rinsing. In Figure 7, we plot V_c during such an experiment for a saturated 40:1 sample ($Q_{max} \approx 5.5$). The original starting V_c directly after rinsing is ~8 μL. However, over the course of a week in an ambient environment, the V_c decreases significantly. For example, V_c decreases to ~5 μL and 1 μL after 1 day and 7 days, respectively (Figure 7, first box). During aging, oil likely leaches out from the network and lubricates the surface, which manifests itself by decreasing V_c. This extra oil near the surface can be rinsed off with water in a second rinse cycle, reverting V_c close to its original value (~7 μL). Again over the course of several days, V_c decreases. This oil leaching behavior is consistent over at least 5 rinsing cycles (Figure 7), with only a small change in the starting V_c. The same slippery property recovery is observed with a highly-swollen ($Q = 7.0$) 50:1 substrate, where $Q_{max} = 9.4$ (Figure S2). To consider if such behavior is limited to Sylgard 184, we also test a PDMS elastomer prepared from Gelest starting materials as a comparison (see methods). Since the starting materials are controlled, we know there are no additional fillers, which may exist in the proprietary Sylgard 184 kit. Our Gelest silicone has a saturated swelling ratio of $Q_{max} = 4.5$, which is between the 30:1 and 40:1 Sylgard 184. By measuring V_c for a saturated Gelest elastomer, we observe the same slippery property recovery after aging for 6 days (Figure S3). These results demonstrate that highly

swollen, low modulus PDMS elastomers have the ability to maintain slipperiness over time and use, and is not limited to the Sylgard 184 kit.

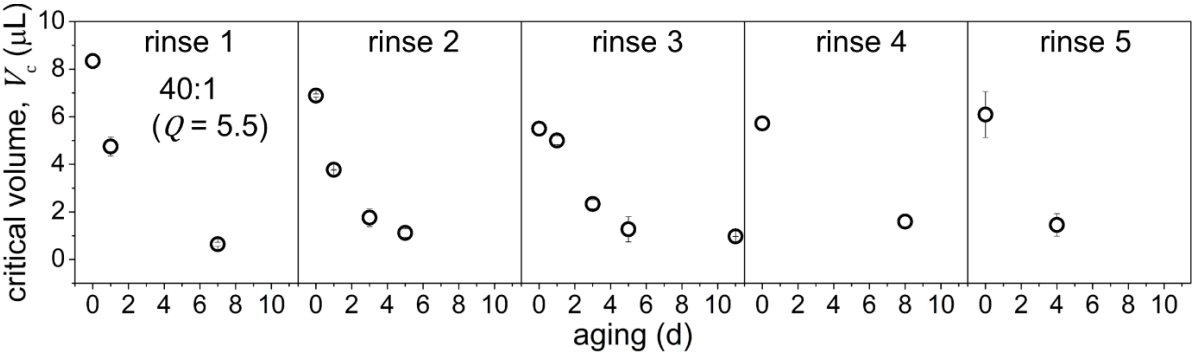

Figure 7. The critical water volume as a function of aging days for a swollen 40:1 ($Q = 5.5$) elastomer. Each box represents one rinse and aging cycle using the same sample.

We hypothesize that an oil layer leaches out to the surface during aging, which is removed during the rinsing process (Figure 8a). Prior literature has shown that oil replenishing can occur at the surface of higher modulus, lubricant infused PDMS substrates.[50,61] To experimentally test whether oil replenishes at the surface of softer, oil-infused materials, we place the PDMS substrate in contact with a piece of standard printer paper for 10 s, and then remove it to see if an oil stain remains. For a rinsed, highly swollen 40:1 sample, no oil stain is transferred to the paper (Figure 8b-8c); this confirms that excess oil is removed during the rinsing process. After 7 days of aging, the substrate is again placed on the paper for 10 s. Upon removing the PDMS, an oil stain remains, indicating there is an extra oil layer on the aged sample (Figure 8d -8e). Although others have utilized an AFM technique to quantify oil layer thicknesses,[22,62] it can be challenging on very soft surfaces. Therefore, we use the oil stain test as an indirect route to observe whether an oil layer exists on the surface.

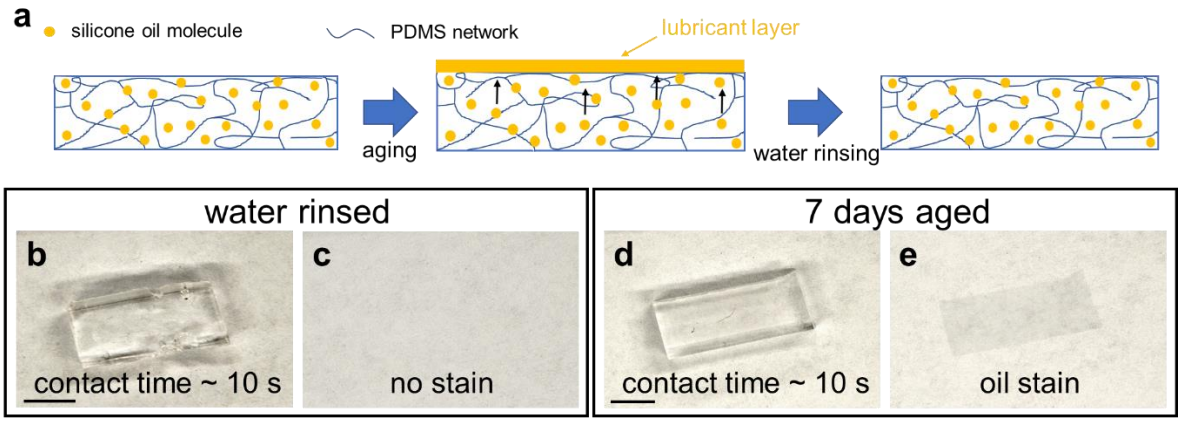

Figure 8. (a) A schematic of rinsing, aging, and re-lubricantion of highly swollen PDMS. (b-e) Paper stain test with a highly swollen 40:1 ($Q = 5.5$) sample. (b-c) A water-rinsed sample and (d-e) a sample aged for 7 days. No stain is left on the paper for water-rinsed samples (c), while an oil stain if observed on the paper for the 7 day aged sample (e). Scale bars: 5 mm.

The fact that imbibed oil migrates to the surface can be explained by the different surface tensions of the PDMS network compared with the low molecular weight silicone oil. The surface tension of PDMS in air is in the range of ~20 to 24 mN/m,[63–65] while the surface tension of low molecular weight silicone oil is 19.7 mN/m (Gelest, Trimethylsiloxy-terminated, 5 cSt).[66] Since the silicone oil has a lower surface tension, we expect it to migrate to surface to cover the elastomer and lower the overall energy. However, once the surface is covered with a thin layer of oil, the oil layer should not continue to increase in thickness, based on a surface energy argument. Recently, Lavielle et al. suggested that further crosslinking of the PDMS network can explain a continuously increasing layer of lubricant in oil-infused silicones.[22] However, our as-prepared samples are first extracted, such that excess crosslinkers and excess uncrosslinked free chains are removed. Hence, the only obvious source of further crosslinking would come from unreacted dangling ends. Since these elastomers are highly swollen, such

that the network chains are expanded, it may not be as likely that these dangling ends are able to react with each other to increase crosslinking; although, we cannot exclude it as a possibility.

Another possible reason for re-lubrication may be due to surface defects, leading to a "defects-driven" mechanism for lubricant separation on the surface of a swollen elastomer. As drawn in Figure 9, the surface of a swollen elastomer may not be perfectly smooth; microcavities may exist on the surface. Inside cavities, a high capillary pressure arises from the high curvatures; the capillary pressure can drive the imbibed oil to separate from the network and fill the cavities through osmo-capillary phase separation.[40] Moreover, an open environment could allow small dust or contaminate particles to land on the surface. These small particulates may also drive oil out from the network through capillarity.[34,35] Driven by small defects or particulates, lubricant would gradually separate from the elastomer and accumulate on the surface. After several days, an apparent lubricant layer would then appear. Overall, it is possible that both continued crosslinking, as well as defect-driven oil separation, can aid in oil re-lubrication in highly swollen surfaces.

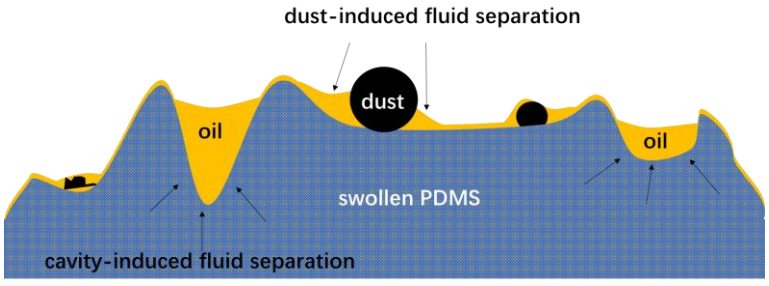

Figure 9. Schematic of a potential mechanism that drive the oil separates from the swollen PDMS

Although oil layer formation is observed in highly swollen samples during aging, such behavior is not observed for an intermediate or low swelling ratio. For example, we measured V_c on a 40:1 sample with a swelling ratio of $Q = 2.1$ (maximum swelling is $Q = 5.5$, which is tested in Figure 8). As illustrated in Figure 10a, the critical volume remains unchanged after leaving it in an ambient environment for over 4 months (134 days) after rinsing. The same paper-staining experiment shows that no oil-stain is transferred to the paper from this sample. Recently, we proposed that strong affinity between the network and the oil can hold the oil inside the network.[32] When the PDMS network is only lightly swollen, the polymer network pressure dominates; this means that oil will remain swollen inside the network, rather than segregate to the interface. This idea is consistent with our findings in Figure 10, in which a layer of oil is not observed during aging.

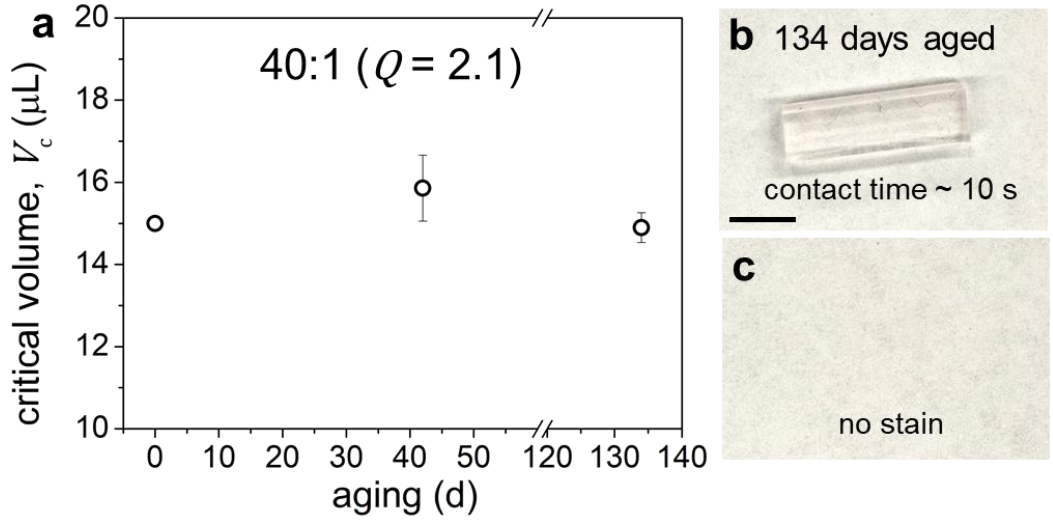

Figure 10. (a) Critical water volume as a function of aging days for 40:1 ($Q = 2.1$) elastomers. For the substrate aged for 134 days, (b) it is put into contact with paper for 10 s, and (c) no stain is left on the paper. Scale bars: 5 mm.

Conclusions

In summary, we investigate the effects of the degree of crosslinking and the degree of swelling on water drop pinning/sliding for soft PDMS elastomers swollen with silicone oil. Our experiments reveal that the critical water drop volume required to slide on a swollen elastomer is mainly controlled by the degree of swelling: Increasing the degree of swelling can dramatically decrease the water drop pinning force. The degree of crosslinking does not strongly affect the critical drop volume when the PDMS base/crosslinker ratio is 40:1 or larger. Contact angle hysteresis decreases with increasing swelling, and is lowest when samples are saturated. Low contact angle hysteresis implies lower adhesion and a more slippery surface. Additionally, we show that highly swollen surfaces display a re-lubrication behavior after rinsing the surface with excess water. Highly swollen samples self-lubricate by generating extra oil on the surface over the course of days, leading to a decrease in the critical drop volume. This oil regeneration at the surface is consistent over multiple rinsing cycles. However, when the degree of swelling is lower, the oil leaching behavior does not occur; the oil remains inside the network rather than segregating to the network-air interface. Overall, our study offers insight into the slippery properties of oil-swollen, low modulus silicone elastomers. Our findings on water drop pinning/sliding aims to inform the design the soft, water-repellent, surfaces.

Methods

PDMS elastomer samples

Sylgard 184 PDMS elastomer preparation

Sylgard 184 elastomers are produced with as-prepared mixtures of 30:1, 40:1, 50:1 and 60:1 by weight of the Sylgard 184 base to curing agent. After mixing and degassing, the mixtures are then poured into a 90 mm × 90 mm square diameter plastic Petri dish and cured in a 65°C pre-heated oven for 48 hours. The as-prepared samples are cut with a razor to a 1 cm by 80 mm size with thickness from 1 mm to 1.5 mm. To extract uncrosslinked free molecules from these samples, the samples are immersed in a beaker of hexane for 1 week while exchanging solvent every two days. Afterwards, the hexane-swollen sample is removed from the beaker and allowed to dry at room temperature. Silicone oil (polydimethylsiloxane, trimethylsiloxy terminated, M_w: 770 g/mol, Gelest) is added directly onto the extracted elastomers. The oil spontaneously swells into the elastomers due to the high affinity between silicone oil and the PDMS network. The swelling ratio is equal to weight of the swollen sample divided by dry (extracted) sample, $Q = w_s/w_d$. The size of final test samples is in the range of 5 mm × 40 mm to 20mm × 140 mm, due to the size changes that occur after the extraction and swelling process. Since the sample volume is large relative to a potential oil layer, this will play a small role in the calculation of Q. Hence, we assume Q remains constant throughout our experiments for a given sample.

Gelest PDMS elastomer preparation

Gelest elastomers are produced by mixing hydride terminated polydimethylsiloxane (Gelest,

DMS-H25) with a chemical crosslinker (Gelest, VDT-5035) and a catalyst (Platinum(0)-1,3-divinyl-1,1,3,3-tetramethyldisiloxane complex solution, Sigma-Aldrich). After mixing and degassing, the mixture is poured into a 35 mm diameter plastic Petri dish and cured in a 65°C pre-heated oven for 48 hours. The extraction and reswelling procedures are same as those for Sylgard 184 sample preparation.

Video recording

Elastomer samples are placed on a vertical post, which is in a chamber with a relative humidity of 70% to 75%. Micropipettes are used to place water drops on the vertical surfaces, and a side-view camera (Chronos 1.4) is used to record drop motion. The video recording rate ranges from 0.2 to 100 fps, depended on the sliding speed of water drops. The recording time ranges from 5 mins to up 8 hours.

Oil stain test

A small block is cut from the PDMS samples for the oil stain tests. PDMS blocks are placed on regular printing paper (Boise, Aspen 30). After being in contact for 10 s, the PDMS blocks are removed from the paper surface. Top view images of the block and paper stain are obtained with a Nikon D610B camera equipped with a Tamron Sp Af 90 mmF/2.8Di Macro Lens.

Advancing and receding contact angles

A goniometer with an automated water dispenser is used to measure the advancing and receding contact angles on the PDMS elastomers. The injecting and withdrawing rate is 0.04 μL/s. The

goniometer pictures are analyzed with ImageJ and using the Contact Angle Plugin to extract macroscale contact angle data.

Modulus

A rheometer (TA Instruments Discovery HR-2) equipped with 8 mm aluminum parallel plates is used to measure the shear modulus of dry and swollen elastomers. The plates are scratched to help with mitigating slip at the plate surfaces. The shear modulus of highly swollen samples is tested to a strain of 1% at a frequency of 0.1 Hz and the dry and slightly swollen samples are tested to a strain of 1% at a frequency of 0.01 Hz (Figure S1). The strains used were confirmed to be in the linear region of a strain sweep up to 10%.[32]

ASSOCIATED CONTENT

Supporting Information. Additional experimental results on critical drop volume on other surfaces, rheological data, and supporting movies of drop pinning/sliding are provided online.

AUTHOR INFORMATION

Corresponding Author

*Email: Jonathan.Pham@uky.edu

Author Contributions

The manuscript was written through contributions of all authors. All authors have given approval to the final version of the manuscript.

ACKNOWLEDGMENTS

This work was primarily funded by the National Science Foundation (NSF, CBET 2043732), and partially supported through the NSF Kentucky EPSCoR (OIA 1849213). The authors also thank Krishnaroop Chaudhuri and Justin Glover for helpful discussion.

REFERENCES

(1) Wang, W.; Lockwood, K.; Boyd, L. M.; Davidson, M. D.; Movafaghi, S.; Vahabi, H.; Khetani, S. R.; Kota, A. K. Superhydrophobic Coatings with Edible Materials. *ACS Appl. Mater. Interfaces* **2016**, *8* (29), 18664–18668. https://doi.org/10.1021/acsami.6b06958.

(2) Tian, X.; Verho, T.; Ras, R. H. A. Moving Superhydrophobic Surfaces toward Real-World Applications. *Science* **2016**, *352* (6282), 142–143. https://doi.org/10.1126/science.aaf2073.

(3) Ramírez-Soto, O.; Sanjay, V.; Lohse, D.; Pham, J. T.; Vollmer, D. Lifting a Sessile Oil Drop from a Superamphiphobic Surface with an Impacting One. *Sci. Adv.* **2020**, *6* (34), 1–11. https://doi.org/10.1126/sciadv.aba4330.

(4) Pan, S.; Guo, R.; Björnmalm, M.; Richardson, J. J.; Li, L.; Peng, C.; Bertleff-Zieschang, N.; Xu, W.; Jiang, J.; Caruso, F. Coatings Super-Repellent to Ultralow Surface Tension Liquids. *Nat. Mater.* **2018**, *17* (11), 1040–1047. https://doi.org/10.1038/s41563-018-0178-2.

(5) Tuteja, A.; Choi, W.; McKinley, G. H.; Cohen, R. E.; Rubner, M. F. Design Parameters for Superhydrophobicity and Superoleophobicity. *MRS Bull.* **2008**, *33* (8),

752–758. https://doi.org/10.1557/mrs2008.161.

(6) Bocquet, L.; Lauga, E. A Smooth Future? *Nat. Mater.* **2011**, *10* (5), 334–337. https://doi.org/10.1038/nmat2994.

(7) Wong, T. S.; Kang, S. H.; Tang, S. K. Y.; Smythe, E. J.; Hatton, B. D.; Grinthal, A.; Aizenberg, J. Bioinspired Self-Repairing Slippery Surfaces with Pressure-Stable Omniphobicity. *Nature* **2011**, *477* (7365), 443–447. https://doi.org/10.1038/nature10447.

(8) Cao, M.; Guo, D.; Yu, C.; Li, K.; Liu, M.; Jiang, L. Water-Repellent Properties of Superhydrophobic and Lubricant-Infused "Slippery" Surfaces: A Brief Study on the Functions and Applications. *ACS Appl. Mater. Interfaces* **2016**, *8* (6), 3615–3623. https://doi.org/10.1021/acsami.5b07881.

(9) Schellenberger, F.; Xie, J.; Encinas, N.; Hardy, A.; Klapper, M.; Papadopoulos, P.; Butt, H. J.; Vollmer, D. Direct Observation of Drops on Slippery Lubricant-Infused Surfaces. *Soft Matter* **2015**, *11* (38), 7617–7626. https://doi.org/10.1039/c5sm01809a.

(10) Preston, D. J.; Lu, Z.; Song, Y.; Zhao, Y.; Wilke, K. L.; Antao, D. S.; Louis, M.; Wang, E. N. Heat Transfer Enhancement during Water and Hydrocarbon Condensation on Lubricant Infused Surfaces. *Sci. Rep.* **2018**, *8* (1), 1–9. https://doi.org/10.1038/s41598-017-18955-x.

(11) Sett, S.; Yan, X.; Barac, G.; Bolton, L. W.; Miljkovic, N. Lubricant-Infused Surfaces for Low-Surface-Tension Fluids: Promise versus Reality. *ACS Appl. Mater. Interfaces* **2017**, *9* (41), 36400–36408. https://doi.org/10.1021/acsami.7b10756.

(12) Preston, D. J.; Song, Y.; Lu, Z.; Antao, D. S.; Wang, E. N. Design of Lubricant

Infused Surfaces. *ACS Appl. Mater. Interfaces* **2017**, *9* (48), 42383–42392. https://doi.org/10.1021/acsami.7b14311.

(13) Wang, N.; Xiong, D.; Deng, Y.; Shi, Y.; Wang, K. Mechanically Robust Superhydrophobic Steel Surface with Anti-Icing, UV-Durability, and Corrosion Resistance Properties. *ACS Appl. Mater. Interfaces* **2015**, *7* (11), 6260–6272. https://doi.org/10.1021/acsami.5b00558.

(14) Rykaczewski, K.; Anand, S.; Subramanyam, S. B.; Varanasi, K. K. Mechanism of Frost Formation on Lubricant-Impregnated Surfaces. *Langmuir* **2013**, *29* (17), 5230–5238. https://doi.org/10.1021/la400801s.

(15) Epstein, A. K.; Wong, T. S.; Belisle, R. A.; Boggs, E. M.; Aizenberg, J. Liquid-Infused Structured Surfaces with Exceptional Anti-Biofouling Performance. *Proc. Natl. Acad. Sci. U. S. A.* **2012**, *109* (33), 13182–13187. https://doi.org/10.1073/pnas.1201973109.

(16) Leslie, D. C.; Waterhouse, A.; Berthet, J. B.; Valentin, T. M.; Watters, A. L.; Jain, A.; Kim, P.; Hatton, B. D.; Nedder, A.; Donovan, K.; Super, E. H.; Howell, C.; Johnson, C. P.; Vu, T. L.; Bolgen, D. E.; Rifai, S.; Hansen, A. R.; Aizenberg, M.; Super, M.; Aizenberg, J.; Ingber, D. E. A Bioinspired Omniphobic Surface Coating on Medical Devices Prevents Thrombosis and Biofouling. *Nat. Biotechnol.* **2014**, *32* (11), 1134–1140. https://doi.org/10.1038/nbt.3020.

(17) Adera, S.; Alvarenga, J.; Shneidman, A. V.; Zhang, C. T.; Davitt, A.; Aizenberg, J. Depletion of Lubricant from Nanostructured Oil-Infused Surfaces by Pendant Condensate Droplets. *ACS Nano* **2020**, *14* (7), 8024–8035. https://doi.org/10.1021/acsnano.9b10184.

(18) Seiwert, J.; Maleki, M.; Clanet, C.; Quéré, D. Drainage on a Rough Surface. *EPL (Europhysics Letters)* **2011**, *94* (1), 16002. https://doi.org/10.1209/0295-5075/94/16002.

(19) Zhang, J.; Wu, L.; Li, B.; Li, L.; Seeger, S.; Wang, A. Evaporation-Induced Transition from Nepenthes Pitcher-Inspired Slippery Surfaces to Lotus Leaf-Inspired Superoleophobic Surfaces. *Langmuir* **2014**, *30* (47), 14292–14299. https://doi.org/10.1021/la503300k.

(20) Cui, J.; Daniel, D.; Grinthal, A.; Lin, K.; Aizenberg, J. Dynamic Polymer Systems with Self-Regulated Secretion for the Control of Surface Properties and Material Healing. *Nat. Mater.* **2015**, *14* (8), 790–795. https://doi.org/10.1038/nmat4325.

(21) Urata, C.; Dunderdale, G. J.; England, M. W.; Hozumi, A. Self-Lubricating Organogels (SLUGs) with Exceptional Syneresis-Induced Anti-Sticking Properties against Viscous Emulsions and Ices. *J. Mater. Chem. A* **2015**, *3* (24), 12626–12630. https://doi.org/10.1039/c5ta02690c.

(22) Lavielle, N.; Asker, D.; Hatton, B. D. Lubrication Dynamics of Swollen Silicones to Limit Long Term Fouling and Microbial Biofilms. *Soft Matter* **2021**, *17* (4), 936–946. https://doi.org/10.1039/d0sm01039a.

(23) Urata, C.; Nagashima, H.; Hatton, B. D.; Hozumi, A. Transparent Organogel Films Showing Extremely Efficient and Durable Anti-Icing Performance. *ACS Appl. Mater. Interfaces* **2021**, *13* (24), 28925–28937. https://doi.org/10.1021/acsami.1c06815.

(24) Chuah, Y. J.; Koh, Y. T.; Lim, K.; Menon, N. V.; Wu, Y.; Kang, Y. Simple Surface Engineering of Polydimethylsiloxane with Polydopamine for Stabilized Mesenchymal

Stem Cell Adhesion and Multipotency. *Sci. Rep.* **2016**, *5* (1), 18162. https://doi.org/10.1038/srep18162.

(25) Tibbitt, M. W.; Anseth, K. S. Hydrogels as Extracellular Matrix Mimics for 3D Cell Culture. *Biotechnol. Bioeng.* **2009**, *103* (4), 655–663. https://doi.org/10.1002/bit.22361.

(26) Zheng, W.; Zhang, W.; Jiang, X. Precise Control of Cell Adhesion by Combination of Surface Chemistry and Soft Lithography. *Adv. Healthc. Mater.* **2013**, *2* (1), 95–108. https://doi.org/10.1002/adhm.201200104.

(27) Kotikian, A.; McMahan, C.; Davidson, E. C.; Muhammad, J. M.; Weeks, R. D.; Daraio, C.; Lewis, J. A. Untethered Soft Robotic Matter with Passive Control of Shape Morphing and Propulsion. *Sci. Robot.* **2019**, *4* (33), 86–1226. https://doi.org/10.1126/scirobotics.aax7044.

(28) Cao, Y.; Tan, Y. J.; Li, S.; Lee, W. W.; Guo, H.; Cai, Y.; Wang, C.; Tee, B. C.-K. Self-Healing Electronic Skins for Aquatic Environments. *Nat. Electron.* **2019**, *2* (2), 75–82. https://doi.org/10.1038/s41928-019-0206-5.

(29) Byun, J.; Lee, Y.; Yoon, J.; Lee, B.; Oh, E.; Chung, S.; Lee, T.; Cho, K.-J.; Kim, J.; Hong, Y. Electronic Skins for Soft, Compact, Reversible Assembly of Wirelessly Activated Fully Soft Robots. *Sci. Robot.* **2018**, *3* (18). https://doi.org/10.1126/scirobotics.aas9020.

(30) Wong, W. S. Y.; Hauer, L.; Naga, A.; Kaltbeitzel, A.; Baumli, P.; Berger, R.; D'Acunzi, M.; Vollmer, D.; Butt, H.-J. Adaptive Wetting of Polydimethylsiloxane. *Langmuir* **2020**, *36* (26), 7236–7245. https://doi.org/10.1021/acs.langmuir.0c00538.

(31) Hönes, R.; Lee, Y.; Urata, C.; Lee, H.; Hozumi, A. Antiadhesive Properties of Oil-Infused Gels against the Universal Adhesiveness of Polydopamine. *Langmuir* **2020**, *36* (16), 4496–4502. https://doi.org/10.1021/acs.langmuir.0c00062.

(32) Cai, Z.; Skabeev, A.; Morozova, S.; Pham, J. T. Fluid Separation and Network Deformation in Wetting of Soft and Swollen Surfaces. *Commun. Mater.* **2021**, *2* (1), 21. https://doi.org/10.1038/s43246-021-00125-2.

(33) Hourlier-Fargette, A.; Antkowiak, A.; Chateauminois, A.; Neukirch, S. Role of Uncrosslinked Chains in Droplets Dynamics on Silicone Elastomers. *Soft Matter* **2017**, *13* (19), 3484–3491. https://doi.org/10.1039/c7sm00447h.

(34) Jensen, K. E.; Sarfati, R.; Style, R. W.; Boltyanskiy, R.; Chakrabarti, A.; Chaudhury, M. K.; Dufresne, E. R. Wetting and Phase Separation in Soft Adhesion. *Proc. Natl. Acad. Sci. U. S. A.* **2015**, *112* (47), 14490–14494. https://doi.org/10.1073/pnas.1514378112.

(35) Pham, J. T.; Schellenberger, F.; Kappl, M.; Butt, H.-J. From Elasticity to Capillarity in Soft Materials Indentation. *Phys. Rev. Mater.* **2017**, *1* (1), 015602. https://doi.org/10.1103/PhysRevMaterials.1.015602.

(36) Sotiri, I.; Tajik, A.; Lai, Y.; Zhang, C. T.; Kovalenko, Y.; Nemr, C. R.; Ledoux, H.; Alvarenga, J.; Johnson, E.; Patanwala, H. S.; Timonen, J. V. I.; Hu, Y.; Aizenberg, J.; Howell, C. Tunability of Liquid-Infused Silicone Materials for Biointerfaces. *Biointerphases* **2018**, *13* (6), 06D401. https://doi.org/10.1116/1.5039514.

(37) Zhang, P.; Zhao, C.; Zhao, T.; Liu, M.; Jiang, L. Recent Advances in Bioinspired Gel Surfaces with Superwettability and Special Adhesion. *Adv. Sci.* **2019**, *6* (18), 1900996.

https://doi.org/10.1002/advs.201900996.

(38) Peppou-Chapman, S.; Hong, J. K.; Waterhouse, A.; Neto, C. Life and Death of Liquid-Infused Surfaces: A Review on the Choice, Analysis and Fate of the Infused Liquid Layer. *Chem. Soc. Rev.* **2020**, *49* (11), 3688–3715. https://doi.org/10.1039/d0cs00036a.

(39) Glover, J. D.; McLaughlin, C. E.; McFarland, M. K.; Pham, J. T. Extracting Uncrosslinked Material from Low Modulus Sylgard 184 and the Effect on Mechanical Properties. *J. Polym. Sci.* **2020**, *58* (2), 343–351. https://doi.org/10.1002/pol.20190032.

(40) Liu, Q.; Suo, Z. Osmocapillary Phase Separation. *Extrem. Mech. Lett.* **2016**, *7*, 27–33. https://doi.org/10.1016/j.eml.2016.02.001.

(41) Hourlier-Fargette, A.; Dervaux, J.; Antkowiak, A.; Neukirch, S. Extraction of Silicone Uncrosslinked Chains at Air-Water-Polydimethylsiloxane Triple Lines. *Langmuir* **2018**, *34* (41), 12244–12250. https://doi.org/10.1021/acs.langmuir.8b02128.

(42) Style, R. W.; Xu, Q. The Mechanical Equilibrium of Soft Solids with Surface Elasticity. *Soft Matter* **2018**, *14* (22), 4569–4576. https://doi.org/10.1039/c8sm00166a.

(43) Park, S. J.; Weon, B. M.; Lee, J. S.; Lee, J.; Kim, J.; Je, J. H. Visualization of Asymmetric Wetting Ridges on Soft Solids with X-Ray Microscopy. *Nat. Commun.* **2014**, *5* (1), 4369. https://doi.org/10.1038/ncomms5369.

(44) Style, R. W.; Dufresne, E. R. Static Wetting on Deformable Substrates, from Liquids to Soft Solids. *Soft Matter* **2012**, *8* (27), 7177–7184. https://doi.org/10.1039/c2sm25540e.

(45) Style, R. W.; Boltyanskiy, R.; Che, Y.; Wettlaufer, J. S.; Wilen, L. A.; Dufresne, E. R.

Universal Deformation of Soft Substrates near a Contact Line and the Direct Measurement of Solid Surface Stresses. *Phys. Rev. Lett.* **2013**, *110* (6), 066103. https://doi.org/10.1103/PhysRevLett.110.066103.

(46) Carré, A.; Gastel, J.-C.; Shanahan, M. E. R. Viscoelastic Effects in the Spreading of Liquids. *Nature* **1996**, *379* (6564), 432–434. https://doi.org/10.1038/379432a0.

(47) Karpitschka, S.; Das, S.; van Gorcum, M.; Perrin, H.; Andreotti, B.; Snoeijer, J. H. Droplets Move over Viscoelastic Substrates by Surfing a Ridge. *Nat. Commun.* **2015**, *6* (1), 7891. https://doi.org/10.1038/ncomms8891.

(48) Zhao, M.; Dervaux, J.; Narita, T.; Lequeux, F.; Limat, L.; Roché, M. Geometrical Control of Dissipation during the Spreading of Liquids on Soft Solids. *Proc. Natl. Acad. Sci. U. S. A.* **2018**, *115* (8), 1748–1753. https://doi.org/10.1073/pnas.1712562115.

(49) Style, R. W.; Hyland, C.; Boltyanskiy, R.; Wettlaufer, J. S.; Dufresne, E. R. Surface Tension and Contact with Soft Elastic Solids. *Nat. Commun.* **2013**, *4* (1), 2728. https://doi.org/10.1038/ncomms3728.

(50) Yao, X.; Dunn, S. S.; Kim, P.; Duffy, M.; Alvarenga, J.; Aizenberg, J. Fluorogel Elastomers with Tunable Transparency, Elasticity, Shape-Memory, and Antifouling Properties. *Angew. Chemie - Int. Ed.* **2014**, *53* (17), 4418–4422. https://doi.org/10.1002/anie.201310385.

(51) Dussan V., E. B. On the Ability of Drops or Bubbles to Stick to Non-Horizontal Surfaces of Solids. Part 2. Small Drops or Bubbles Having Contact Angles of Arbitrary Size. *J. Fluid Mech.* **1985**, *151*, 1–20.

https://doi.org/10.1017/S0022112085000842.

(52) Extrand, C. W.; Kumagai, Y. Liquid Drops on an Inclined Plane: The Relation between Contact Angles, Drop Shape, and Retentive Force. *J. Colloid Interface Sci.* **1995**, *170* (2), 515–521. https://doi.org/10.1006/jcis.1995.1130.

(53) Smith, J. D.; Dhiman, R.; Anand, S.; Reza-Garduno, E.; Cohen, R. E.; McKinley, G. H.; Varanasi, K. K. Droplet Mobility on Lubricant-Impregnated Surfaces. *Soft Matter* **2013**, *9* (6), 1772–1780. https://doi.org/10.1039/c2sm27032c.

(54) Sedev, R. V.; Petrov, J. G.; Neumann, A. W. Effect of Swelling of a Polymer Surface on Advancing and Receding Contact Angles. *J. Colloid Interface Sci.* **1996**, *180* (1), 36–42. https://doi.org/10.1006/jcis.1996.0271.

(55) ElSherbini, A. I.; Jacobi, A. M. Retention Forces and Contact Angles for Critical Liquid Drops on Non-Horizontal Surfaces. *J. Colloid Interface Sci.* **2006**, *299* (2), 841–849. https://doi.org/10.1016/j.jcis.2006.02.018.

(56) ElSherbini, A. I.; Jacobi, A. M. Liquid Drops on Vertical and Inclined Surfaces: I. An Experimental Study of Drop Geometry. *J. Colloid Interface Sci.* **2004**, *273* (2), 556–565. https://doi.org/10.1016/j.jcis.2003.12.067.

(57) Gao, N.; Geyer, F.; Pilat, D. W.; Wooh, S.; Vollmer, D.; Butt, H. J.; Berger, R. How Drops Start Sliding over Solid Surfaces. *Nat. Phys.* **2018**, *14* (2), 191–196. https://doi.org/10.1038/nphys4305.

(58) Chen, X.; Wen, G.; Guo, Z. What Are the Design Principles, from the Choice of Lubricants and Structures to the Preparation Method, for a Stable Slippery Lubricant-Infused Porous Surface? *Mater. Horizons* **2020**, *7* (7), 1697–1726.

https://doi.org/10.1039/d0mh00088d.

(59) Baumli, P.; D'Acunzi, M.; Hegner, K. I.; Naga, A.; Wong, W. S. Y.; Butt, H.-J.; Vollmer, D. The Challenge of Lubricant-Replenishment on Lubricant-Impregnated Surfaces. *Adv. Colloid Interface Sci.* **2021**, *287*, 102329. https://doi.org/10.1016/j.cis.2020.102329.

(60) Kreder, M. J.; Daniel, D.; Tetreault, A.; Cao, Z.; Lemaire, B.; Timonen, J. V. I.; Aizenberg, J. Film Dynamics and Lubricant Depletion by Droplets Moving on Lubricated Surfaces. *Phys. Rev. X* **2018**, *8* (3), 31053. https://doi.org/10.1103/PhysRevX.8.031053.

(61) Yeong, Y. H.; Wang, C.; Wynne, K. J.; Gupta, M. C. Oil-Infused Superhydrophobic Silicone Material for Low Ice Adhesion with Long-Term Infusion Stability. *ACS Appl. Mater. Interfaces* **2016**, *8* (46), 32050–32059. https://doi.org/10.1021/acsami.6b11184.

(62) Peppou-Chapman, S.; Neto, C. Mapping Depletion of Lubricant Films on Antibiofouling Wrinkled Slippery Surfaces. *ACS Appl. Mater. Interfaces* **2018**, *10* (39), 33669–33677. https://doi.org/10.1021/acsami.8b11768.

(63) Grundke, K.; Michel, S.; Knispel, G.; Grundler, A. Wettability of Silicone and Polyether Impression Materials: Characterization by Surface Tension and Contact Angle Measurements. *Colloids Surfaces A Physicochem. Eng. Asp.* **2008**, *317* (1–3), 598–609. https://doi.org/10.1016/j.colsurfa.2007.11.046.

(64) Tian, Y.; Ina, M.; Cao, Z.; Sheiko, S. S.; Dobrynin, A. V. How to Measure Work of Adhesion and Surface Tension of Soft Polymeric Materials. *Macromolecules* **2018**, *51* (11), 4059–4067. https://doi.org/10.1021/acs.macromol.8b00738.

(65) Ina, M.; Cao, Z.; Vatankhah-Varnoosfaderani, M.; Everhart, M. H.; Daniel, W. F. M.; Dobrynin, A. V.; Sheiko, S. S. From Adhesion to Wetting: Contact Mechanics at the Surfaces of Super-Soft Brush-like Elastomers. *ACS Macro Lett.* **2017**, *6* (8), 854–858. https://doi.org/10.1021/acsmacrolett.7b00419.

(66) Gelest. *Silicone Fluids: Stable Inert Media*; 2012.

Table of Contents (TOC) graphic